REVISTA DE MATEMÁTICA: TEORÍA Y APLICACIONES 2016 **23**(1) : 155–172
CIMPA – UCR ISSN: 1409-2433 (PRINT), 2215-3373 (ONLINE)

COMBINING NEURAL NETWORKS AND GEOSTATISTICS FOR LANDSLIDE HAZARD ASSESSMENT OF SAN SALVADOR METROPOLITAN AREA, EL SALVADOR

COMBINANDO REDES NEURONALES Y GEOESTADÍSTICA PARA EVALUACIÓN DE DESLIZAMIENTOS DE TIERRA DEL ÁREA METROPOLITANA DE SAN SALVADOR, EL SALVADOR

RICARDO RÍOS[*] ALEXANDRE RIBÓ[†] ROBERTO MEJÍA[‡]
GIOVANNI MOLINA[§]

Received: 19 Feb 2014; Revised: 28 Aug 2015; Accepted: 29 Sep 2015

[*]Department of Mathematics, Science and Mathematics Faculty, University of El Salvador, El Salvador. E-Mail: ricardo.sv@gmail.com

[†]National Institute of Health, Ministry of Health of El Salvador, El Salvador. E-Mail: alexandre4rt@gmail.com

[‡]Misma dirección que/*Same address as*: A. Ribó. E-Mail: robertomejia1685@gmail.com

[§]Ministry of Environment and Natural Resources of El Salvador, El Salvador. E-Mail: giova.molina@gmail.com

Abstract

This contribution describes the creation of a landslide hazard assessment model for San Salvador, a department in El Salvador. The analysis started with an aerial photointerpretation from Ministry of Environment and Natural Resources of El Salvador (MARN Spanish acronym), where 4792 landslides were identified and georeferenced along with 7 conditioning factors including: geomorphology, geology, rainfall intensity, peak ground acceleration, slope angle, distance to road, and distance to geological fault. Artificial Neural Networks (ANN) were utilized to assess the susceptibility to landslides, achieving results where more than 80% of landslide were properly classified using in-sample and out of sample criteria. Logistic regression was used as base of comparison. Logistic regression obtained a lower performance. To complete the analysis we have performed interpolation of the points using the kriging method from geostatistical approach. Finally, the results show that is possible to derive a landslide hazard map, making use of a combination of ANNs and geostatistical techniques, thus the present study can help landslide mitigation in El Salvador.

Keywords: landslide; hazard assessment; El Salvador; ANN; geostatistics; artificial neural networks; kriging.

Resumen

Esta contribución describe la creación de un modelo de evaluación de deslizamiento de tierra para el Área Metropolitana de San Salvador, departamento de El Salvador. El análisis inició con la obtención de una foto aérea del Ministerio de Medio Ambiente y Recursos Naturales (MARN) en donde 4792 deslizamientos fueron identificados y georeferrenciados junto con 7 factores condicionantes incluyendo: geomorfología, geología, precipitaciones máximas, aceleraciones sísmicas, pendiente del terreno, distancia a carretera y falla geológica. Redes Neuronales Artificiales (RNA) fueron utilizadas para la evaluación de la susceptibilidad a deslizamiento de tierra, logrando que más del 80% de deslizamientos fueran apropiadamente clasificados usando un criterio dentro y fuera de la muestra con la que se estimaron los parámetros del modelo. Regresión Logística fue usada como base de comparación, obteniendo este modelo un rendimiento inferior. Para completar el análisis se realizó la interpolación de puntos usando el método kriging proveniente del enfoque geoestadístico. Finalmente, los resultados muestran que es posible obtener un mapa de riesgo a deslizamiento de tierra, haciendo uso de una combinación de RNA y técnicas geoestadísticas con lo cual la presente investigación puede ayudar a la mitigación de deslizamientos de tierra en El Salvador.

Palabras clave: deslizamiento de tierra; evaluación de riesgo; El Salvador; RNA; geoestadística.

Mathematics Subject Classification: 62P12.

1 Introduction

El Salvador, one of the smallest and most crowded nations in Central America, extends in Pacific coast about 240 km westward from the Gulf of Fonseca to the border with Guatemala (see Fig. 1). El Salvador has an active subduction boundary between Cocos and Caribbean plates located 30 km offshore. Therefore, El Salvador is affected with high seismicity and volcanic activity related to this active boundary. There are two main sources of seismic activity: the upper interface thrust that coincides with the location of the recent volcanoes, and the Benioff-Wadaty zones of subducted Cocos plate where deeper intraplate earthquakes occurs [16]. Due to this tectonic and volcanic activity, El Salvador has rugged relief. The main ranges cross the country with a rough west-east trend, parallel to the coastline. These are separated from each other by faults and grabens. These ranges present several highly active volcanoes. The surface geology in El Salvador is almost entirely volcanic, dominated by upper Tertiary to Holocene volcanic rocks. Only sparse outcrops of sedimentary and plutonic rocks are located in the northern ranges, in the border with Honduras [42]. Some of the most recent volcanic layers are formed by poorly consolidated ashes and highly erodible tuffs [6].

Throughout the year, the country experiences a tropical climate with two seasons: a dry season (November to April) and wet season (May to October). The climate of El Salvador is generally warm. In the dry season there is very little rainfall; but during rainy seasons, heavy showers take place. Periodically El Salvador is affected by tropical storms and occasionally by hurricanes.

As in other parts of Central America, landslides in El Salvador constitute an important natural hazard due to prevailing steep terrain covered with poorly consolidated volcanic materials, and the frequent occurrence of extreme precipitation events and intense earthquakes. This problem is exacerbated by the extreme deforestation and the consequent high level rates of erosion. Poverty, overpopulation and uncontrolled urbanization characterize the Salvadoran human settlements, which makes El Salvador a country with high landslide risks. An example of this high risk was the devastating effect of Las Colinas landslides, triggered by a major earthquake (Mw 7.6) on January 13th, 2001 in Santa Tecla, a major city located close to San Salvador, the Salvadoran capital[19]. A huge amount of soil mass (about 200,000 m^3) was thrown off the rim of El Balsamo range, and destroyed many houses causing more than 500 deaths. Together with this event, several landslides ocurred along the country, especially in the Metropolitan Area of San Salvador (MASS) [25]. Another example is the large number of heavy-rainfall induced landslides occurred during Hurricane Mitch on October and November 1998 [14].

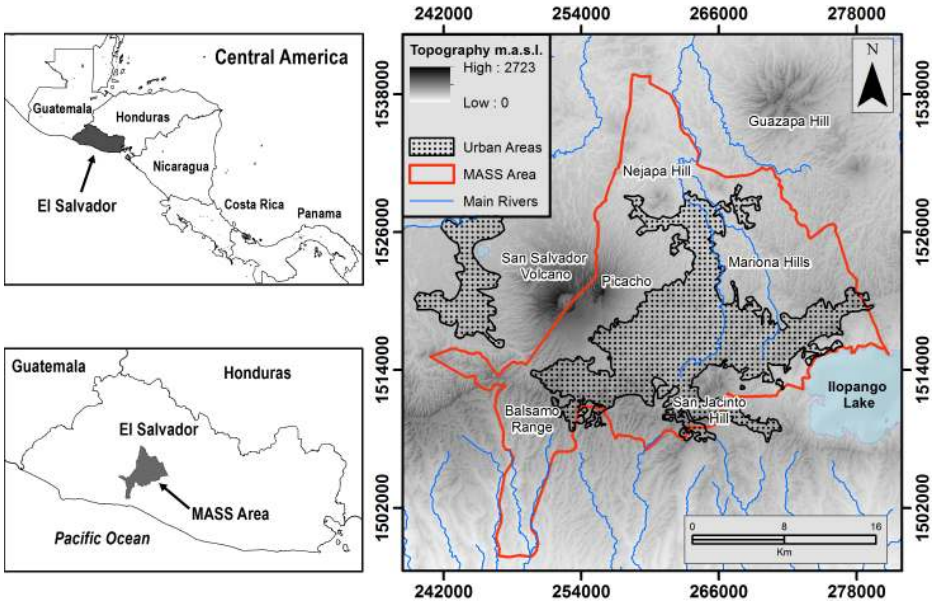

Figure 1: Location of El Salvador in Central America, map of El Salvador with location of the Metropolitan Area of San Salvador (MASS) and its topography.

Due to the above, it is necessary to implement mechanisms that allow us to quantify the hazard of a given geographic area to landslides. Usually this is done with development of susceptibility maps, which present in a graphical way the zones more susceptible to landslides, and represent a practical tool for urban planning. We propose an Artificial Neural Network model (ANN), which is a family of statistical learning models inspired on biological neural networks. The model proposed is used to estimate the susceptibility to landslide. From the results obtained by the model, a map was derived using kriging, which is a method of spatial interpolation from the geostatistical approach.

2 Brief state of art

Since the pioneering work shown in [9], several mathematical and statistical models have been proposed to model landslide susceptibility: deterministic models ([8], [32], and [31]) and probabilistic models ([7], [13], and [26]).

Popular classification models have been used, such as logistic regression ([1], [23], and [21]), neural networks ([22], [29],[44], [18], and [43]), and support vector machines ([3] and [39]).

According to [40], the magnitude of a possible slide is difficult to foresee as it depends on the magnitude of the triggering event and the environmental conditions (e.g., height of water table) at the moment of the event. Because of these complex relationships between the dependent variable and causal factors, and since neural networks are particularly useful for detecting complex non-linear relationships in large datasets, we chose this kind of model, despite the disadvantages such as greater computational burden and tendency to overfit.

3 Study area

MASS is formed by 14 municipalities among them is San Salvador, the capital of the country. It has 587 km^2 and according to the most recent census [30] it has 1,566,629 inhabitans with a density of population of 2669 hab/km2. Geographically, MASS is extended over a flat erosional surface (650-760 m.a.s.l.), gently sloping to the east towards Ilopango Caldera also known as Ilopango Lake. MASS is bordered to the south by the Balsamo Range and San Jacinto Hill, to the west by San Salvador volcano and Mariona Hills (refer to Fig. 1). Human settlement is not restricted to the plain and it spreads up to surrounding heights and volcano flanks.

All rocks exposed in MASS have volcanic origin and consist of intercaled primary and reworked deposits from Late Tertiary to Holocene age [36]. The younger ones are known as Tierra Blanca pyroclastic ash deposits and form a relative continuous layer in the majority of MASS with an average thickness of 4 m [36]. These are deposits derived mainly from Ilopango Caldera eruptions with more than 50 m of thick [36]. Tierra Blanca soils are highly susceptible to erosion. One of the most common dangerous effects of the erosion in this area are landslides during heavy rainfall and earthquake ground shaking [36]. Chávez et al. [11] identified high and moderate erosion hazard in the majority of MASS area. The more recent layer Tierra Blanca, known as Tierra Blanca Joven (TBJ) [24] presents very poor geotechnical properties, especially when there is an increment of soil moisture (i.e. during rainy seasons). This results in high instability and susceptibility ([10] and [34]). Several incised rivers and ravines cross MASS area. Due to the large erosion rates of the area, natural slopes of these watercourses are often close to vertical and can reach heights of over 10 m. Taking into account this property of volcanic soils, usually vertical slopes are cut to urban and road construction. As Bommer & Rodriguez [6] identified in Central America, although such slopes may remain stable for years, they may become unstable, abruptly and totally under the action of heavy rainfall or seismic shaking. Hernández [24] carried out a detailed description of this process in

TBJ, where these instabilities are very common. In the study area fault trends are characterized by steep angles (65°- 90°). The main fault system is characterized by an east-west trend; this trend is responsible for the steep northern slope of the El Balsamo Range. The other fault systems have north, northwest, and northeast trends and are more active in the present tectonic setting [36]. However, all the mentioned fault families appear active. Thus the several fault systems were formed at different times, but were repeatedly reactivated [35]. Finally there are also several ringlike faults that can be related to subsurface collapse due to volcanic tectonic subsidence [36]. The last eruption of San Salvador volcano was in 1917. The majority of the magma's total volume (97%) extruded from several vents in the northwest flank of the volcano, outside of MASS. However, a fraction of MASS is located under the proximal volcanic hazard zone according to Sofield [38]. In the steep slopes of San Salvador volcano, especially at Picacho, the highest peak which is located in the eastern side, there is a high lahar hazard that threatens MASS [27]. In addition to that one of the most destructive eruptions in the world history was 430 A.D. The TBJ eruption was produced by the Ilopango Caldera and according to Dull [17], yielded total devastation in whole MASS area.

4 Landslide inventory and data sources of input variables

The Landslide inventory was developed by the Ministry of Environment and Natural Resources (MARN Spanish acronym) and it was conducted in two stages. The first was carried out based on fieldwork after the 2001 earthquakes in El Salvador. The second stage consisted of a visual inventory of places where landslides were identified through satellite image from IRS-C sensor (Indian) in the same year.

Once the landslide inventory was finished, 4792 landslides were identified, 0.5% of the total points georeferenced. In addition to the landslide information, the following data sources of input variables was provided by MARN:

1. **Geomorphology:** Refers to landforms that result from lithospheric dynamics of geographic area. This variable was obtained in the project of national land use plan in El Salvador. It is unpublished geomorphologic cartography in digital format provided by MARN.

2. **Slope:** Slope gradient is an important component and a preparatory cause of landsliding [21]. It was calculated from digital elevation model (DEM) provided by MARN (scale 1:100,000).

3. **Geology:** Description of the geology of the area according to digital geological map of El Salvador (scale 1:100,000) [42].

4. **Rainfall intensity:** From the precipitation database compiled by the MARN's weather stations for the period 1970-2001, maximum precipitations were obtained, and then, a contour map was generated through kriging interpolation method.

5. **Peak ground accelaration:** Maximum ground acceleration expressed in Gal for a return period of 500 years. This data was obtained from the evaluation of seismic Hazard in Central America carried out under the framework of RSIS II project [4].

6. **Road distance:** Distance in kilometers to the nearest road. Road map was obtained from digital national map created by Centro Nacional de Registros de la República de El Salvador (CNR).

7. **Fault distance:** Distance in kilometers to the nearest fault. This information was obtained from the digital geological map of El Salvador (scale 1:100,000) [42].

5 Artificial neural network model for discrete choice

Logistic regression represents a neural network with a neuron in the hidden layer, whose output is dichotomous. The following adapted form of the Multilayer Perceptron (MLP) may be used for modeling binary classification problems. In equation (1) $x_{k,i}$ are the observed values in the ith input variables belonging to the kth case. The expressions $w_{j,k}$ and λ_j showed in equations (1) and (3) are the parameters of the model.

$$n_{j,i} = w_{j,0} + \sum_{k=1}^{k^*} w_{j,k} x_{k,i} \tag{1}$$

$$N_{j,i} = \frac{1}{1 + \exp^{-n_{j,i}}} \tag{2}$$

$$p_i = \sum_{j=1}^{j^*} \lambda_j N_{j,i} \tag{3}$$

$$\sum_{j=1}^{j^*} \lambda_j = 1, \lambda_j \geq 0. \tag{4}$$

In equation (3) p_i is the output of a neural network with k^* input characteristics and j^* neurons. In the context of the present study, p_i represents the probability of landslide ocurrence.

Before estimating the parameters of the neural network model, it is necessary to standardize the input variables. In particular for classification problems is more suitable to scale inputs to $[-1, 1]$ rather than $[0, 1]$ [41]. The following scaling was applied to each input variable:

$$z = \frac{x - \bar{x}}{\sigma_x}. \tag{5}$$

In equation (5) z is the new variable transformed. $\bar{x}$ and σ_x are the mean and the standard deviation of the input variable to transform, respectively.

The method used for estimating the parameters of the model was a hybrid method [28]. Firstly, a genetic algorithm was implemented in a package developed in the R statistical software [33] to obtain a good estimation of the parameters of the model. The R package can be accessed from the following Web address: `https://goo.gl/PHaaG2`

After obtaining a good estimate by genetic algorithms, this was used as an initial guess value for the conjugate gradient method implemented in the R statistical software (optim function), to obtain a better estimation of the parameters of the model.

6 Spatial prediction

Estimating spatial correlation

In standard statistical problems, correlation can be estimated from a scatterplot, when several data pairs x, y are available. The spatial correlation between two observations of a variable $z(s)$ at locations s_1 and s_2 cannot be estimated because only a single pair is available. To estimate spatial correlation from observational data, it is necessary to make stationarity assumptions before we can make any progress. One commonly used form of stationarity is intrinsic stationarity, which assumes that the process that generated the samples is a random function $Z(s)$ composed of a mean and residual [5] as follows:

$$Z(s) = \mu + \delta(s) \tag{6}$$

with a constant mean

$$E\left(Z(s)\right) = \mu \tag{7}$$

and a variogram defined as

$$\lambda(h) = \frac{1}{2} E\left(Z(s) - Z(s+h)\right)^2. \tag{8}$$

Ordinary kriging in terms of the covariance function

The predictor assumption is

$$\hat{Z(s_0)} = \sum_{i=1}^{n} w_i Z(s_i). \tag{9}$$

It is a weighted average of the sample values, and $\sum_{i=1}^{n} w_i = 1$ to ensure unbiasedness. The w_i's are the weights that will be estimated. Kriging minimizes the expression (10) which is the mean squared error of prediction [12].

$$\min \sigma_e^2 = E\left[Z(s_0) - \hat{Z(s_0)}\right]^2. \tag{10}$$

7 Results

The data were randomly divided into three sub-samples: The first was used for the estimation of the parameters of the neural network model (training set), the second was used to choose the model with more generalization capability (validation set), and the last was used to evaluate how well the model is able to generalize data not used in the estimation process (test set).

To determine the number of neurons in the hidden layer, the method of trial and error was used, starting with few neurons and progressively increasing the number of neurons in the hidden layer. Table 1 summarizes how well the models fit on the training, validation, and test sets.

The model with 17 neurons in the hidden layer was chosen because it had the best performance in the validation set. After that, a logistic regression model was fitted as a basis of comparison. Table 2 shows logistic regression results. Clearly, the neural network model chosen has better performance than the logistic regression model.

To generate the map of landslide hazards, the following steps were followed based on geostatistics methodology: Exploratory analysis, Variogram modelling and Spatial prediction using ordinary kriging, validation, and exporting the spatial predictions to raster format.

Developed to perform the previous steps, an R script was developed. This script can be downloaded in: `https://goo.gl/3N8n99`

Table 1: Summary of classification accuracy on the training, validation, and test sets for neural network models.

	Percentage score		
Number of neurons	Train set	Validation set	Test set
2	0.7011	0.7020	0.7124
3	0.7206	0.7072	0.7401
4	0.7425	0.7197	0.7458
5	0.7601	0.7604	0.7740
6	0.7823	0.7704	0.7604
7	0.7853	0.7704	0.7763
8	0.7942	0.7865	0.7878
9	0.8009	0.7871	0.7901
10	0.8321	0.8132	0.8009
11	0.8194	0.7792	0.7542
12	0.8230	0.8006	0.8159
13	0.8408	0.8006	0.8031
14	0.8373	0.8017	0.8127
15	0.8517	0.8210	0.8247
16	0.8246	0.8017	0.8028
17	0.8543	0.8283	0.8246
18	0.8467	0.8022	0.8418
19	0.8341	0.7991	0.8274

First of all, one thousand and fifty georeferenced points with their probability of occurrence calculated using neural network were selected randomly for the map generation process, leaving the others for validation of the kriging model. The Exploratory analysis showed the presence of spatial correlation. This was done making scatter plot of pairs $Z(s_i)$ and $Z(s_j)$, grouped according to their separation distance. Furthermore, the data did not show the presence of anisotropic effect.

Regarding variogram estimation, the spherical, gaussian and exponential models were proposed. Using cross-validation methodology, the best model was the exponential, since it had an $R^2 = 0.42$ against $R^2 = 0.40$ and $R^2 = 0.39$ of the models spherical and gaussian, respectively. Using the exponential model, spatial predictions were calculated on a grid of 1500 $\times$ 1500 and exported to Geotiff raster format. Finally, Geographic Information System (ArcGIS® of ESRI) was used to design the final map (Figure 2). This map (Fig. 2) represents the landslide probability of occurrences in MASS. According to Fig. 2,

Table 2: Summary of classification accuracy on the training, validation and test sets for logistic regression.

	Percentage score		
Model	Train set	Validation set	Test set
logistic regression	0.6710	0.6748	0.663

higher probability of landslide occurrence are around 0.8. These are located in the northern slopes of Balsamo Range (western side of MASS), in the eastern slope of San Salvador volcano and Picacho, along the extension of Mariona Hills and in the southeastern side, between Ilopango lake and San Jacinto Hill. Areas with lower probability are located in southern and western side of Nejapa Hill, in the north-east of the studied area, in the northern banks of Ilopango lake, in northeast slope of San Salvador Volcano, in the surrounding areas of San Jacinto Hill, and in general in southern side of MASS.

8 Discussion and conclusions

A landslide hazard assessment study was carried out in Metropolitan Area of San Salvador (MASS). The study started with the construction of a landslide inventory and analysis of the causal factors related to the occurrences of landslide. The problem of modeling landslide is very complex, and for this reason the study proved the efficacy of the neural network model with a percentage of correct classification of around 80% against other models such as logistic regression with a percentage of correct classification under 70%.

In the process of estimating the weights of the model, a heuristic technique was used to obtain a better solution after a local search was used. The difficulty of this approach is due to the intensive computation involved in the estimation of a neural network model, which takes between 4 and 10 hours. For this reason, the statistical significance of the input variables could not be assessed by means of bootstrapping (a statistical resampling technique). For all of the above, parallel computing must be used rather than serial computing to estimate weights of the neural networks models.

The results obtained through geostatistical methodology met the assumptions for kriging method application. A final map of landslide probability of occurrence (see Fig. 2) generated by kriging method was the result of multidisciplinary work, which implied an intense geological analysis (i.e. MARN inventory of 4792 landslides), together with the use of sophisticated statistical techniques. This landslide hazard map is a user-friendly tool to evaluate landslide

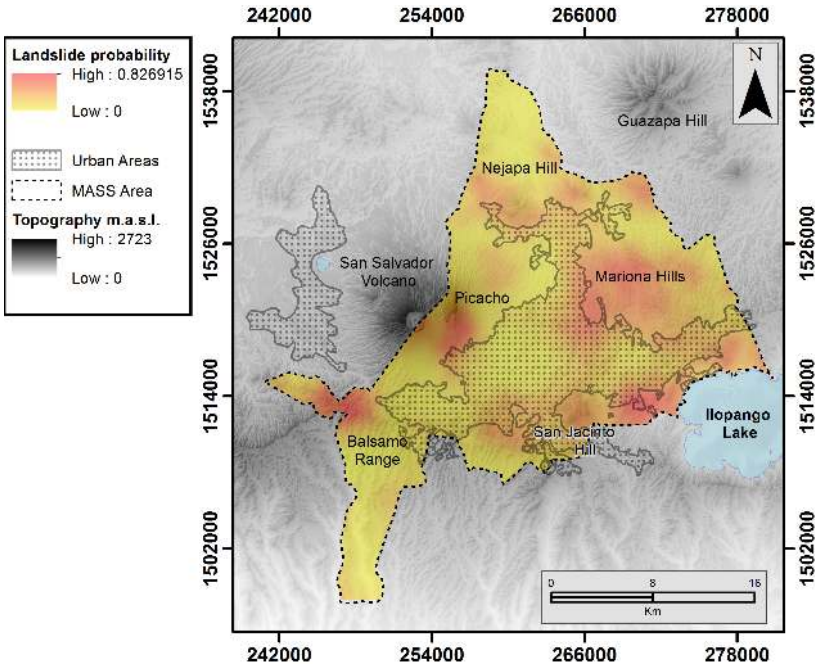

Figure 2: Landslide hazard map MASS where the landslide probability of occurrence is shown.

risk in MASS and can be useful for many purposes such as territorial planning, prevention and landslide mitigation, and so on.

High probability of landslide occurrence in Picacho slope implies very high risk due to the proximity of urban areas and the large volume of mobilized materials. Major et al.[27] identified in San Salvador volcano lahars as voluminous as 2 million of m^3 that can affect large zones of urban areas. Southern areas of MASS also have a high risk of landslides that is similar to Las Colinas landslide which involved a total volume of around 200,000 m^3 [19]. A similar risk exists in the northern slope of Balsamo range and San Jacinto Hill, affecting very crowded urban areas.

The present hazard landslide map is consistent with former landslide hazard maps carried out in the region using approaches conceptually different. Fernández-Lavado et al.[20] presented a landslide hazard GIS map of MASS generated through a bivariate statistical method considering several conditioning factors showing similar hazard areas. The only differences are located mainly in the

Nejapa Hill and San Jacinto Hill where Fernández-Lavado et al. [20] identified a slightly higher hazard, and the area between San Jacinto Hill and Ilopango Lake where the former study presented a hazard slightly lower. Since landslides are an erosional phenomenon, the highest probability areas of landslide occurrence coincide with the areas with highest hazard of erosion in the erosion hazard map of MASS proposed by Chávez et al. [11]. There are similarities with susceptibility hazard maps at national scale generated through logistic regression [21], artificial neural network [22], and Mora-Vahrson [37]. However the high landslide areas are more extended in these national maps than the present study. These differences could be explained by the working scale. Other possible explanation can be related to the data. This present work was built using a more extended landslide catalog and more up-to-date data (e.g. seismic hazard evaluation from Benito et al. [4]) than former works, so that this map is more detailed because it is at regional scale.

Rock falls were not included in the catalog; these were very common during 2001 earthquakes in El Balsamo Range [25]. On the other hand, the seismic microzonation of MASS will improve the estimation of peak ground acceleration. The local geologic conditions are responsible for the modifications (amplification, frequency content, and duration) experimented by seismic motions just before reaching the ground surface. Additionally, the geometry of the ground surface also may produce amplification (topographic effects) [2]. These effects can be important in soft soils close to incised rivers and also in San Salvador volcano, Balsamo ranges and hills. Crosta et al. [15] identified an amplification factor of 1.3–1.4 in Las Colinas failure area (Balsamo Ranges). All these variables can improve the predictive ability of the model and the likelihood of landslides.

Acknowledgment

The authors are indebted with MARN for providing the data and Geographic Information System software such as ILWIS and ArcGIS® of ESRI.

References

[1] Akgun, A. (2012) "A comparison of landslide susceptibility maps produced by logistic regression, multi criteria decision, and likelihood ratio methods: a case study at Izmir, Turkey", *Landslides* **9**(1): 93–106.

[2] Aki, K. (1993) "Local site effects on weak and strong ground motion", in: F. Lund (Ed.) *New Horizons in Strong Motion: Seismic Studies and Engineering Practice*, *Tectonophysics* **218**(1): 93–111.

[3] Ballabio, C.; Sterlacchini, S. (2012) "Support vector machines for landslide susceptibility mapping: the Staffora river basin case study, Italy", *Mathematical Geosciences* **44**(1): 47–70.

[4] Benito, M.B.; Lindholm, C.; Camacho, E.; Climent, Á.; Marroquín, G.; Molina, E.; Rojas, W.; Escobar, J.J.; Talavera, E.; Alvarado, G.E.; Torres, Y. (2012) "A new evaluation of seismic hazard for the Central America region", *Bulletin of the Seismological Society of America* **102**(2): 504–523.

[5] Bivand, R.S.; Pebesma, E.J.; Gomez-Rubio, V.; Pebesma, E.J. (2008) *Applied Spatial Data Analysis with R*. Springer, New York.

[6] Bommer, J.J.; Rodriguez, C.E. (2002) "Earthquake-induced landslides in Central America", *Engineering Geology* **63**(3): 189–220.

[7] Campbell, R.H.; Brookshire, D.S.; Bernknopf, R.L.; Shapiro, C.D. (1988) "A probabilistic approach to landslide hazard mapping in Cincinnati, Ohio, with application for economic evaluation", *Bulletin of the Association of Engineering Geologists* **25**(1): 39–56.

[8] Capparelli, G.; Versace, P.P. (2013) "Landslide susceptibility from mathematical model in Sarno area", *Hydrology and Earth System Sciences Discussions* **10**(10): 12643–12662.

[9] Carrara, A. (1983) "Multivariate models for landslide hazard evaluation", *Journal of the International Association for Mathematical Geology* **15**(3): 403–426.

[10] Chávez J.A.; Landaverde J.M.; Ayala O.E.; Mendoza L.E. (2014) "Application of constitutive models in the volcanic tephra "Tierra Blanca Joven", *Ingeniería* **24**(2): 53–78.

[11] Chávez, J.A.; Sebesta, J.; Kopecky, L.; López, R. (2014) "Application of geomorphologic knowledge for erosion hazard mapping", *Natural Hazards* **71**(3): 1323–1354.

[12] Christou, N. (2013) "Ordinary kriging in terms of the covariance function", in: `http://goo.gl/0J1RkO`, consulted 23-Jun-2013, 5:30 p.m.

[13] Chung, C.J.F.; Fabbri, A. G. (2003). "Validation of spatial prediction models for landslide hazard mapping", *Natural Hazards* **30**(3): 451–472.

[14] Crone, A.J.; Baum, R.L.; Lidke, D.J.; Sather, D.N.D.; Bradley, L.A.; Tarr, A.C. (2002) "Landslides Induced by Hurricane Mitch in El Salvador-An Inventory and Description of Selected Features", Preprint, USGS Open File Report 01-444, available in `http://pdf.usaid.gov/pdf_docs/Pnacr105.pdf`

[15] Crosta, G. B.; Imposimato, S.; Roddeman, D.; Chiesa, S.; Moia, F. (2005) "Small fast-moving flow-like landslides in volcanic deposits: the 2001 Las Colinas Landslide (El Salvador)", *Engineering geology* **79**(3): 185–214.

[16] Dewey, J.W.; White, R.A.; Hernández, D.A. (2004) "Seismicity and tectonics of El Salvador", *Geological Society of America Special Papers* **375**: 367–378.

[17] Dull, R.A. (2004) "Lessons from the mud, lessons from the Maya: Paleoecological records of the Tierra Blanca Joven eruption", *Geological Society of America Special Papers* **375**: 237–244.

[18] Ermini, L.; Catani, F.; Casagli, N. (2005) "Artificial neural networks applied to landslide susceptibility assessment", *Geomorphology* **66**(1): 327–343.

[19] Evans, S.G.; Bent, A.L. (2004) "Las Colinas landslide, Santa Tecla: A higly destructive flowslide triggered by January 13, 2001, El Salvador earthquake", *Geological Society of America Special Papers* **375**: 25–37.

[20] Fernández-Lavado, C.; Sánchez, A.; Amenós, M.; Barrio, J. (2008) "Caracterización de la susceptibilidad y de la amenaza por movimientos de ladera del Área Metropolitana de San Salvador (AMSS). Scale 1: 75000 (1 Sheet)", Preprint, Project IPGARAMSS framework. Geólogos del Mundo. San Salvador, El Salvador.

[21] García-Rodríguez, M.J.; Malpica, J.A.; Benito, B.; Díaz, M. (2008) "Susceptibility assessment of earthquake-triggered landslides in El Salvador using logistic regression", *Geomorphology* **95**(3): 172-191.

[22] García-Rodríguez, M.J.; Malpica, J.A. (2010) "Assessment of earthquake-triggered landslide susceptibility in El Salvador based on an Artificial Neural Network model", *Natural Hazards and Earth System Science* **10**(6): 1307–1315.

[23] Gaskill, J.; Zuber, B.; Nordman, E. (2015) "Analyzing landslide susceptibility in St. Vincent and the Grenadines using co-kriging and logistic regression", Preprint, The 2015 IMAGIN Award, Michigan United States. Presentation available in: `http://www.imagin.org/awards/sppc/2015/papers/jacob_gaskill_presentation.pdf`

[24] Hernández, W.E. (2004) *Características Geomecánicas y Vulcanologicas de las Tefras Tierra Blanca Joven, Caldera de Ilopango, El Salvador*. M.Sc. Thesis, Universidad Politécnica de Madrid–Universidad Politécnica de El Salvador.

[25] Jibson, R.W.; Crone, A.J.; Harp, E.L.; Baum, R.L.; Major, J.J.; Pullinguer, C.R.; Escobar, D.; Martinez, M: Smith, M.E. (2004) "Landslides triggered by the 13 January and 13 February 2001, earthquakes", *Geological Society of America Special Papers* **375**: 69–88.

[26] Lee, S.; Choi, J.: Min, K. (2004) "Probabilistic landslide hazard mapping using GIS and remote sensing data at Boun, Korea", *International Journal of Remote Sensing* **25**(11): 2037–2052.

[27] Major, J.J.; Chilling, S.P.; Pullinguer, C.R.; Escobar, C.D. (2004) "Debris-flow hazards at San Salvador, San Vicente, and San Miguel volcanoes, El Salvador", *Geological Society of America Special Papers* **375**: 89–108.

[28] McNelis, P.D. (2005) *Estimation of a Network with Evolutionary Computation*. Academic Press, New York.

[29] Melchiorre, C.; Abella, E. C.; van Westen, C. J.; Matteucci, M. (2011) "Evaluation of prediction capability, robustness, and sensitivity in non-linear landslide susceptibility models, Guantánamo, Cuba", *Computers & Geosciences* **37**(4): 410–425.

[30] Ministerio de Economía–Dirección General de Estadística y Censos (2013) "VI Censo de Población y V de Vivienda", El Salvador, in: `http://goo.gl/yvjzPy`, consulted 23-Dec-2013, 2:30 p.m.

[31] Neuhäuser, B.; Damm, B.; Terhorst, B. (2012) "GIS-based assessment of landslide susceptibility on the base of the weights-of-evidence model", *Landslides* **9**(4): 511–528.

[32] Pradhan, B.; Oh, H.; Buchroithner, M. (2010) "Weights-of-evidence model applied to landslide susceptibility mapping in a tropical hilly area", *Geomatics, Natural Hazards and Risk* **1**(3): 199–223.

[33] R Core Team. (2014) *R: A Language and Environment for Statistical Computing*. Vienna: R Foundation for Statistical Computing.

[34] Rolo, R.; Bommer, J.J.; Houghton, B.F.; Vallance, J.W.; Berdousis, P.; Mavrommati, C.; Morphy, W. (2004) "Geologic and engineering characterization of Tierra Blanca pyroclastic ash deposits", *Geological Society of America Special Papers* **375**: 55–68.

[35] Rymer, M.J. (1987) "The San Salvador earthquake of October 10, 1986-geologic aspects", *Earthquake Spectra* **3**(3): 435–463.

[36] Schmidt-Thomé M. (1975) "The geology in the San Salvador area (El Salvador, Central America), a basis for city development and planning", *Geologisches Jahrbuch* **13**: 207–228.

[37] SNET-MARN, Servicio Nacional de Estudios Territoriales-Ministerio de Ambiente y Recursos Naturales (2013) "Memoria técnica para el mapa de susceptibilidad de deslizamientos de tierra en El Salvador", in: `http://www.snet.gob.sv/ver/geologia/susceptibilidad+actual/`, consulted 12-Sep-2013, 2:30 p.m.

[38] Sofield, D. (2004) "Eruptive history and volcanic hazards of Volcan San Salvador", *Geological Society of America Special Papers* **375**: 147–158.

[39] Tien Bui, D.; Pradhan, B.; Lofman, O.; Revhaug, I. (2012) "Landslide susceptibility assessment in Vietnam using support vector machines, decision tree, and naive Bayes models", *Mathematical Problems in Engineering* **2012**, 26 pp. Available in: `http://www.hindawi.com/journals/mpe/2012/974638/`

[40] Van Westen, C.J.; Van Asch, T.W.; Soeters, R. (2006) "Landslide hazard and risk zonation why is it still so difficult?", *Bulletin of Engineering Geology and the Environment* **65**(2): 167–184.

[41] Warren, S. (2002) "Neural network FAQ", in: `ftp://ftp.sas.com/pub/neural/FAQ.html`, consulted 10-Jan-2014, 10:30 a.m.

[42] Weber, H.S.; Wiesemann, G.; Lorenz, W.; Schmidt-Thomé, M. (1978) "Mapa geológico de la República de El Salvador", Preprint, Bundesanstalt für Geowissenschaften und Rohstoffe, Hannover, Germany.

[43] Yesilnacar, E.; Topal, T. (2005) "Landslide susceptibility mapping: A comparison of logistic regression and neural networks methods in a medium

scale study, Hendek region (Turkey)", *Engineering Geology* **79**(3): 251–266.

[44] Zeng-Wang, X.U. (2001) "GIS and ANN model for landslide susceptibility mapping", *Journal of Geographical Sciences* **11**(3): 374–381.